The challenge of simulating the sensitivity of the Amazonian clouds microstructure to cloud condensation nuclei number concentrations

Pascal Polonik[1,*], Christoph Knote[1], Tobias Zinner[1], Florian Ewald[2], Tobias Kölling[1], Bernhard Mayer[1], Meinrat O. Andreae[3,4], Tina Jurkat-Witschas[4], Thomas Klimach[4], Christoph Mahnke[5,6], Sergej Molleker[5], Christopher Pöhlker[4], Mira L. Pöhlker[4], Ulrich Pöschl[4], Daniel Rosenfeld[7], Christiane Voigt[2,6], Ralf Weigel[6], and Manfred Wendisch[8]

[1]Meteorologisches Institut, Ludwig Maximilians-Universität München, Munich, Germany
[2]Institut für Physik der Atmosphäre, Deutsches Zentrum für Luft- und Raumfahrt (DLR), Oberpfaffenhofen, Germany
[3]Scripps Institution of Oceanography, University of California at San Diego, La Jolla, California, USA
[4]Multiphase Chemistry and Biogeochemistry Departments, Max Planck Institute for Chemistry, Mainz, Germany
[5]Particle Chemistry Department, Max Planck Institute for Chemistry, Mainz, Germany
[6]Institut für Physik der Atmosphäre, Johannes Gutenberg-Universität, Mainz, Germany
[7]Institute of Earth Sciences, Hebrew University of Jerusalem, Jerusalem, Israel
[8]Leipziger Institut für Meteorologie, Universität Leipzig, Leipzig, Germany
[*]*now at:* Scripps Institution of Oceanography, University of California at San Diego, La Jolla, California, USA

Correspondence: Christoph Knote (christoph.knote@physik.uni-muenchen.de)

Abstract. The realistic representation of cloud-aerosol interactions is of primary importance for accurate climate model projections. The investigation of these interactions in strongly contrasting clean and polluted atmospheric conditions in the Amazon region has been one of the motivations for several field observations, including the airborne Aerosol, Cloud, Precipitation, and Radiation Interactions and DynamIcs of CONvective cloud systems - Cloud Processes of the Main Precipitation Systems in Brazil: A Contribution to Cloud Resolving Modeling and to the GPM (Global Precipitation Measurement) (ACRIDICON-CHUVA) campaign based in Manaus, Brazil in September 2014. In this work we combine in situ and remotely sensed aerosol, cloud, and atmospheric radiation data collected during ACRIDICON-CHUVA with regional, online-coupled chemistry-transport simulations to evaluate the model's ability to represent the indirect effects of biomass burning aerosol on cloud microphysical properties (droplet number concentration and effective radius).

We found agreement between modeled and observed median cloud droplet number concentrations (CDNC) for low values of CDNC, i.e., low levels of pollution. In general, a linear relationship between modeled and observed CDNC with a slope of two was found, which means a systematic overestimation of modeled CDNC as compared to measurements. Variability in cloud condensation nuclei (CCN) number concentrations and cloud droplet effective radii (r_{eff}) was also underestimated by the model.

Modeled effective radius profiles began to saturate around 500 CCN $\mathrm{per\,cm^3}$ at cloud base, indicating an upper limit for the model sensitivity well below CCN concentrations reached during the burning season in the Amazon Basin. Regional background aerosol concentrations were sufficiently high such that the additional CCN emitted from local fires did not cause a notable change in modelled cloud microphysical properties.

In addition, we evaluate a parameterization of CDNC at cloud base using more readily available cloud microphysical properties. Our study casts doubt on the validity of regional scale modeling studies of the cloud albedo effect in convective, polluted situations where the number concentration of CCN is greater than 500 cm^{-3}.

1 Introduction

Aerosol particles influence the formation of cloud droplets, and thereby the microphysical and macrophysical properties of clouds. Cloud droplet sizes and number concentrations determine the effect of clouds on atmospheric radiation and, therefore, also on weather and climate. Increased aerosol concentrations increase the cloud albedo (Twomey, 1991) and possibly the lifetime (Albrecht, 1989) of clouds by decreasing droplet size if the total liquid water mass is assumed constant. Cloud alterations by aerosol (i.e. indirect effects) can therefore lead to enhanced reflection of solar radiation under high aerosol loading, and therefore cause a net cooling of the sub-cloud layer. However, the magnitude of these effects is not well constrained, which causes major uncertainties in current climate projections (IPCC, 2014).

Representing aerosol-cloud interactions in numerical models that form the basis of these projections is challenging because two of the most dynamic and complex atmospheric systems (aerosol and clouds) must be adequately represented individually before considering an accurate representation of their interactions (Ghan et al., 2016). Correctly modeling cloud condensation nucleii (CCNs) number concentration requires accurate representation of aerosol chemistry and size, which depend on parameterizations of emissions, relevant chemical reactions, microphysical interactions like coagulation, and removal processes like dry deposition (Zaveri et al., 2008). In sufficiently complex parameterizations the calculated CCNs will then influence the formation of droplets under saturated conditions and conversely, the droplets may remove the aerosol from the atmosphere.

Cloud microphysical parameterizations with varying levels of complexity have been incorporated into numerical models of the atmosphere (e.g., Khain and Sednev, 1996; Seifert and Beheng, 2006; Morrison et al., 2005; Grützun et al., 2008; Thompson and Eidhammer, 2014), which provides opportunities to better understand the underlying physical processes. It is difficult, however, to disentangle benefits in forecast-relevant quantities (e.g., 500 hPa pressure field deviation, storm track accuracy, or accumulated precipitation) from an actual improvement in the modelled cloud macro- and microphysical characteristics and its impact on the atmospheric radiation budget. Testing such parameterizations on a mechanistic level requires direct comparisons of model output to a variety of data sources (Seinfeld et al., 2016) as well as situations in which a noticeable aerosol signal can be expected. Events like volcanic eruptions (Malavelle et al., 2017; McCoy and Hartmann, 2015), desert dust outbreaks (Levin et al., 2005; Sassen et al., 2003), or wildfires (Rosenfeld, 1999; Brioude et al., 2009) provide strong signals that facilitate such process-level analysis of aerosol-cloud interactions.

We focus on the Amazon, which has been a historically popular location for aerosol-cloud investigations, largely because both very high and very low aerosol concentrations can exist in the region and because convective clouds are somewhat

predictable. There have been multiple efforts to quantify Amazonian aerosol-cloud interactions from remote sensing (Kaufman and Nakajima, 1993; Kaufman and Fraser, 1997; Lin et al., 2006; Wall et al., 2014), in situ measurements (Andreae et al., 2004; Martin et al., 2017; Andreae et al., 2018), combinations of measurement types (Rosenfeld et al., 2012; Gonçalves et al., 2015), and models (Feingold et al., 2005; Zhang et al., 2008; Martins et al., 2009). However, few studies have attempted to combine analysis of regional numerical models with measurememnts (Ten Hoeve et al., 2011). The specific comparison of modeled and measured microphysical quantities have previously not been done. Aerosol-cloud parameterizations and computational power have recently improved to allow for such a study, but the direct comparison of modeled and measured cloud parameters remains challenging.

We use simulations and novel measurements from a recent field campaign in the Amazon to explore aerosol-cloud-radiation effects of biomass burning from a microphysical perspective. We first evaluate whether numerical simulations on convection-permitting scales can accurately represent observed cloud microphysical properties. For this purpose we focus on cloud droplet number concentration (CDNC) and cloud droplet effective radius (r_{eff}) vertical profiles, since r_{eff} profiles represent the microphysical development of a cloud and can be derived from in situ and remote sensing observations.

Though r_{eff} profiles describe the vertical evolution of cloud microphysical properties, it is actually the number of activated cloud condensation nuclei at cloud base, N_{a}, that provides the link between cloud development and aerosol availability (Khain et al., 2005). Parameterizations have been developed to determine N_{a} based on observations of r_{eff} since N_{a} is a somewhat elusive quantity to observe using remote sensing (Rosenfeld et al., 2012). Therefore we then also evaluate the applicability of the parameterization from Freud et al. (2011) using in situ, remote-sensing and model-derived r_{eff} profiles along with modeled and measured N_{a}.

Though many measurements and modeling studies have focused on the Amazon, they have not attempted to directly compare regional model output and measured cloud microphyical parameters. This comparison is a step towards bridging the gap between the observations used to improve physical understanding and the numerical models used to predict future climate.

2 Methods

2.1 Field Campaign

The Aerosol, Cloud, Precipitation, and Radiation Interactions and DynamIcs of CONvective cloud systems - Cloud Processes of the Main Precipitation Systems in Brazil: A Contribution to Cloud Resolving Modeling and to the GPM (Global Precipitation Measurement) (ACRIDICON-CHUVA) field campaign (Wendisch et al., 2016), was conducted over the Amazon in September 2014 during the dry season, when biomass burning from regional agricultural practices creates strong perturbations of cloud condensation nuclei (CCN) number concentration (Pöhlker et al., 2018). Researchers collected data on aerosol size and composition, CCN concentration, cloud phase and droplet size, and trace gas concentrations, and other atmospheric quantities. Both remote sensing and in situ data were collected aboard the High Altitude and Long Range Research Aircraft (HALO), operated by the German Aerospace Center (DLR). HALO flew underneath and within clouds to reconstruct vertical profiles. Typically, HALO research flights began with a ferry from Manaus to a region of interest, followed by sampling in that

Table 1. Dates of flights conducted during the ACRIDICON-CHUVA campaign, with basic information about each flight compiled from Wendisch et al. (2016) and the campaign blog (https://acridicon-chuva.weebly.com/; last accessed: July 10, 2018). CCN levels during each research flight are binned into low ("+"), medium ("++") and high ("+++").

Date	Flight #	CCN level	Description
2014-09-11	AC09	+	Clean conditions for cloud profiling
2014-09-12	AC10	+	Satellite coordination and several in situ clouds sampled in relatively clean conditions
2014-09-16	AC11	++	Tracer experiment near Manaus, with some fires in the vicinity
2014-09-18	AC12	+++	Polluted conditions but relatively few large clouds sampled
2014-09-19	AC13	+++	Polluted conditions, sampling of complete cloud profiles
2014-09-21	AC14	++	Satellite coordination, GoAmazon GI aircraft coordination, medium pollution
2014-09-23	AC15	++	Surface albedo measurement early, cloud sampled later, medium pollution
2014-09-25	AC16	++	Tracer experiment near Manaus, fires in the vicinity
2014-09-27	AC17	+++	Sample clouds over different land surfaces, compare to GPM satellite, polluted conditions
2014-09-28	AC18	+	Medium sized cumulus samples and full cloud profiles in clean conditions

region, and ending with the trip back to Manaus (Figure 1, Table 1). The regions of interest were areas with forecasted presence of convective clouds above specific surface conditions, such as intact forest or polluted agricultural burning areas. Many of the HALO flights were conducted in regions where medium or high aerosol number concentrations from biomass burning were suspected to influence cloud microphysical and radiative properties.

2.2 Model

We attempted to reproduce the measurements conducted during the HALO flights using numerical simulations with the Weather Research and Forecasting model with Chemistry (WRF-Chem, Grell et al., 2005) at convection-permitting scales. The model simulated atmospheric motion with online calculations of trace gases and aerosol chemical and physical properties in a nested domain setup. One degree resolution, six-hourly updated meteorological boundary conditions were taken from analyses of the National Center For Environmental Prediction Global Forecast System (NCEP GFS), and chemical boundary conditions were provided by forecasts of the global chemistry model MOZART (https://www.acom.ucar.edu/wrf-chem/mozart.shtml, last accessed February 6th, 2018).

The simulations feature a size-resolved description of the full lifecycle of ambient aerosol, including biomass burning emissions, secondary particle formation through trace gas oxidation, and dry and wet deposition. Specifically, we used the Model for OZone And Related chemical Tracers (MOZART) gas-phase chemistry (Emmons et al., 2010; Knote et al., 2014) and the Model for Simulating Aerosol Interactions and Chemistry (MOSAIC) aerosol module (Zaveri et al., 2008), with a volatility basis set parameterization for organic aerosol evolution (Knote et al., 2015). Anthropogenic emissions data were taken from the Emissions Database for Global Atmospheric-Research from the task force for Hemispheric Transport of Air Pollution

(EDGAR-HTAP, Janssens-Maenhout et al., 2012). Biogenic emissions are calculated online using the Model of Emissions of Gases and Aerosols from Nature (MEGAN, Guenther et al., 2006). The Fire Inventory from NCAR (FINN) module was used for the fire emissions data (Wiedinmyer et al., 2011).

Radiative properties of the aerosol population are considered based on size distribution and component-resolved optical properties (Barnard et al., 2010). The modeled aerosol description is linked to the double-moment microphysics scheme of Morrison and Gettelman (2008), and no convection parameterization was applied in the nested domain. The Morrison and Gettelman (2008) scheme has five hydrometeor classes (cloud droplets, rain, cloud ice, snow, and graupel), with each size distribution parameterized by a Gamma function. The cloud droplet effective radius is calculated through integration over the droplet size distribution:

$$r_{eff} = \frac{\int_0^\infty r^3 N(r) \mathrm{d}r}{\int_0^\infty r^2 N(r) \mathrm{d}r} \tag{1}$$

with r cloud droplet radius, and $N(r)$ droplet number concentration at radius r.

Effects of aerosol particles on atmospheric radiation (direct effect) are considered as presented in Fast et al. (2006). The number of CCN available for cloud formation as well as their physiochemical properties (size distribution and hygroscopicity) are provided to the cloud microphysics scheme based on the online-calculated aerosol properties. Activation of aerosol particles as cloud droplets is calculated based on the aerosol size distribution and chemical composition using κ-Koehler theory (Abdul-Razzak and Ghan, 2000, 2002), with relevant aspects of the implementation in the version of WRF-Chem used here presented in Gustafson Jr et al. (2007) and Chapman et al. (2009). The life cycle of activated aerosol particles is modelled explicitly; i.e., they are removed from the interstitial aerosol population and their evolution is modelled in accordance with that of the cloud droplets in which they are incorporated, including processes like washout from precipitation or re-evaporation. Secondary, in-cloud activation of aerosol particles to cloud droplets is only considered to the extent that entrainment and in-cloud supersaturation is represented on the grid-scale. Cloud chemistry and limited heterogeneous processes are included as presented in Knote et al. (2015). Chemistry and aerosol processes are included in an operator-splitting fashion, in which individual processes update model fields sequentially. For each WRF-Chem time step, advection is calculated first, followed by droplet activation and then chemistry and aerosol processes.

The above-described WRF-Chem simulations were conducted over the Amazon region for the ACRIDICON-CHUVA mission period between 8 - 30 September 2014. A continuous simulation with 15 km horizontal resolution, covering an area of approximately 3000 $\times$ 2700 km^2 (200 $\times$ 180 grid points), and 36 vertical levels up to 50 hPa, was conducted for the full campaign period (see Figure 1 for domain overview). To keep the large-scale meteorology in line with reality, WRF-Chem was restarted every 24 hours (at 0 hours UTC) from GFS analyses. Concentrations of trace gases and aerosol quantities were carried over, however, to allow for multi-day pollution build-up and aging. Each 24 hour period was simulated with a 6 hour meteorological spin-up with nudging and a chemical restart file from the previous day. Meteorology was then allowed to evolve freely within the WRF-Chem domain (i.e. no nudging was applied) to enable the model to develop the implemented

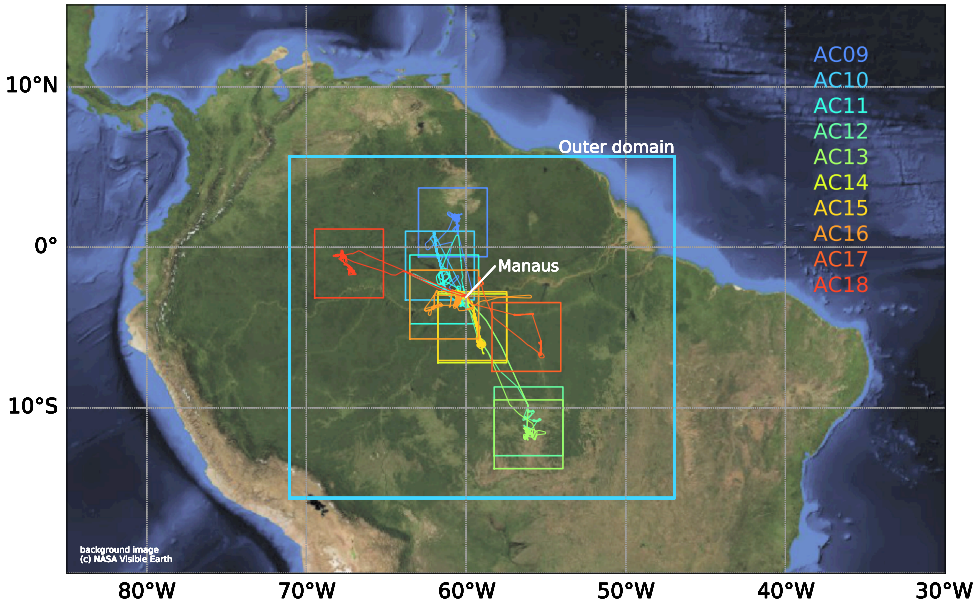

Figure 1. A map showing the campaign area, with all ACRIDICON-CHUVA research flights considered in this study as color-coded lines, the continuously-run outer simulation domain (blue box) as well as the individual nested domains used for analysis of each research flight, identified by the flight labels (Table 1). The outer domain resolution is 15 km and the inner domain resolution is 3 km.

aerosol-cloud-interactions. Three additional days before the study period were simulated to spin-up trace gas chemistry and aerosol.

Convection-permitting, 3 km horizontal resolution domains (180 × 180 grid points, approx. 540 × 540 km^2) were then "nested" into this simulation during days with HALO flights. Two-way interactions were allowed between the parent and the nested domains. The location of these "nests" varied and were chosen so that they covered the area of interest sampled by HALO in each flight (Figure 1, see also Section 3.1). On each flight day, the nested domain was started (by interpolating the current state of the outer domain) at 09:00 UTC and run until 21:00 UTC, hence covering the full time frame of each HALO research flight. All model results presented in this study are from the nested, convection-permitting domains.

2.3 Measurements

2.3.1 Cloud in situ measurements

The cloud combination probe (CCP) combines the cloud imaging probe (CIP) and the cloud droplet probe (CDP) to measure the cloud particle size distribution by detecting their forward-scattered laser light (Lance et al., 2010). During the ACRIDICON-CHUVA campaign, the CCP measured at 1 Hz frequency from underneath the right wing of the HALO aircraft (Wendisch et al., 2016). A correction for the high flight velocities was applied to improve data quality (Weigel et al., 2016). The CCP measures particles with diameters between 2 - 960 µm, but here we only used the 14 bins for particle diameters from 3 - 50 µm

(from the CDP) to calculate the cloud particle effective radius. Except for the details of the selection of appropriate data points, the data used here is the same as described in Braga et al. (2017a). To filter the data we calculated liquid water content from binned effective diameter measurements and only included those with at least 1 $\mathrm{g\,kg^{-1}}$ liquid water content. This threshold is consistent with the one used to define "cloudy" points in model output.

Like the CCP-CDP, the Cloud and Aerosol Spectrometer with Depolarization (CAS-DPOL) measures cloud particle size distributions at 1 Hz frequency (Baumgardner et al., 2011; Voigt et al., 2017). The CAS-DPOL measures the intensity of forward-scattered light between 4 - 12 $\mathrm{degrees}$ in 30 size bins from particles with diameter 0.5 - 50 $\mu\mathrm{m}$. The polarized backward-scattered light is used to analyze the sphericity and thermodynamic phase of the measured particles (Baumgardner et al., 2014; Järvinen et al., 2016), but this capability was not used for our analysis. Our calculation of the cloud particle effective radius (Schumann et al., 2017) was again limited to particles between 3 - 50 $\mu\mathrm{m}$, which corresponds to 10 Mie-ambiguity corrected size bins, to account for consistency with the CDP. Further details on CAS-DPOL data evaluation are given in Kleine et al. (2018).

Profiles of r_{eff} were derived using data from both the CAS-DPOL and the CDP. Braga et al. (2017a) demonstrated that the CDP and CAS-DPOL instruments are comparable within their expected measurement uncertainties. Flamant et al. (2018) and Taylor et al. (2019) also found good agreement between CAS-DPOL and CDP measurements in shallow clouds. Here, we combine measurements from both instruments into one in situ dataset to construct effective radii profiles. Therefore, the concentration of activated cloud condensation nuclei N_{a}, is derived using all in situ r_{eff} measurements with their respective adiabatic liquid water content (see further description in Section 2.3.4). Treating in situ measurements from the two instruments as independent is justifiable in part because they are located on opposite wings of the aircraft.

2.3.2 CCN in situ measurements

The number concentration of CCN was measured with a continuous-flow streamwise thermal gradient CCN counter (CCNC, model CCN-200, DMT, Longmont, CO, USA) (Roberts and Nenes, 2005; Rose et al., 2008). Activated CCN that grow to a diameter of at least 1 $\mu\mathrm{m}$ at a set water vapor supersaturation between 0.1 - 5$\%$ are counted by the instrument at 1Hz. Two sample inlets were used during the ACRIDICON-CHUVA campaign, but here we only use data from the HALO aerosol submicron inlet (HASI), which collected data at a constant supersaturation of 0.55 $\%$. The uncertainty of the CCN measurements is dominated by the counting statistics and ranges between 10$\%$ for high CCNs and 20$\%$ for low CCNs (Krüger et al., 2014). The supersaturation uncertainty is also about 10$\%$ (Braga et al., 2017a).

2.3.3 Cloud remote sensing measurements

The spectral imager of the Munich Aerosol and Cloud Scanner (specMACS) was installed on the HALO aircraft during ACRIDICON-CHUVA. specMACS is a hyperspectral line camera that measures at visible and near-infrared wavelengths (Ewald et al., 2016). Marshak et al. (2006) and Martins et al. (2011) suggested using the solar radiation reflected by illuminated cloud sides to derive the vertical profile of effective radius and cloud phase, but the ACRIDICON-CHUVA campaign was the first time that passive cloud side remote sensing was applied systematically for a large number of cases. Zinner et al.

(2008) and Ewald et al. (2018) developed a cloud side retrieval and demonstrated the application using ACRIDICON-CHUVA data. Jäkel et al. (2017) derived phase information from cloud-side reflectivity measurements during ACRIDICON-CHUVA. specMACS was mounted on HALO at a sideward viewing port to observe clouds passed by the aircraft. Cloud vertical profiles were then retrieved using the method by Ewald et al. (2018) along the flight route akin to a push-broom satellite instrument. Results for three cases are compared to in situ and WRF-Chem model data.

specMACS cases shown in this paper are first example cases and mainly presented to showcase the capability of airborne remote sensing to provide effective radius profiles and cloud droplet number concentration (CDNC). They are not representative for whole flights or flight regions as the used in situ or modelled data, but show specific example local situations along a few minutes of flight time. In this respect they complement the large scale picture provided by modelled data averaged over $540 \times 540\ \mathrm{km}^2$ or the in situ data collected over several hours flight time. specMACS cloud scenes were selected based on favorable data collection conditions. This includes minimal turning of the aircraft, favorable sunlight conditions, and high cloud coverage.

2.3.4 Derivation of N_a from in situ, remote sensing, and model cloud data

The central quantity to determine the influence of aerosol on cloud development and lifetime is the number of activated cloud condensation nuclei at cloud base, N_a (e.g. Khain et al., 2005; Freud et al., 2011). During ACRIDICON-CHUVA, HALO directly sampled N_a during their cloud profile flights, providing a valuable comparison to remotely sensed and modeled data. As the collection of in situ data is expensive and spatial coverage is limited, Rosenfeld et al. (2012) suggested to infer N_a at cloud base using other more readily available observations like satellite retrievals. Freud et al. (2011) proposed a parametrization that derives N_a from the vertical profile of droplet radii. To do this, cloud base temperature and pressure are first used to calculate an adiabatic liquid water content (LWC_a) under the assumption that all water vapor above the saturation vapor pressure is condensed during the moist adiabatic ascent of a parcel. Then, LWC_a can be combined with an empirical relation between r_eff and the volumetric radius, r_v (i.e., $r_\mathrm{v} = 1.08 \cdot r_\mathrm{eff}$ as in Freud et al. (2011)), and the density of water ρ_w to derive a fixed N_a:

$$N_a = \frac{1}{\rho_w} \cdot \frac{3}{4\pi} \cdot \frac{LWC_a}{r_\mathrm{v}^3} \cdot 0.7 \tag{2}$$

The ratio of LWC_a and r_v^3 is found as the slope of a linear regression through all available point pairs of LWC_a and r_v^3 in the droplet size profile, forced through the origin. An additional mixing factor of 0.7 accounts for the imperfection of the adiabatic assumption (Freud et al., 2011; Braga et al., 2017a). Freud et al. (2011) empirically derived this factor using in situ effective radius and LWC data from multiple previous field campaigns, including one in the Amazon. Although there was geographic diversity in the data used for the derivation, only one estimation was made which may introduce an unknown error in our studies. This could be especially relevant for remotely sensed data that measure cloud sides rather than a cloud cross-section. Nonetheless, we apply the same derivation and same mixing factor to all three available r_eff datasets: remotely sensed, in

situ, and model output. Applying this method to multiple data sources provides insights into the validity of this concept. The resulting N_{a} can also be used for direct comparison of the different input r_{eff} profiles.

3 Representation of cloud microphysics in the model

3.1 Deriving comparable quantities for model-measurement evaluation

Comparing the three different sources of information on cloud microphysical properties (model, remote-sensing, and in situ observations) is not straightforward. Colocating in situ and remote-sensing observations required observing a cloud using the side-facing specMACS, and then flying into this cloud to obtain respective in situ measurements. During ACRIDICON-CHUVA, cloud clusters had been identified for each research flight, which were then passed several times to allow for remote-sensing observations before probing these clusters in situ. This precludes direct comparison of individual clouds without diligent data selection, but allows for a statistical comparison of in situ data collected near the cluster and the corresponding remote-sensing observations. Simulations will not reproduce an individual (observed) cloud, but they will create a comparable, realistic regional environment with comparable clouds. Hence, the nested domains were chosen such that they are center on the cloud cluster chosen as target for an ACRIDICON-CHUVA research flight. Assuming a homogeneous environment within the model domain, a statistical comparison of all modelled clouds in the model domain with observations taken of the cloud cluster within the domain is reasonable. Therefore, we used all clouds within the respective nested model domain to derive model statistics. Observation statistics are based on all data collected within the spatial domain of the model nest. As mentioned above, statistics pertaining to in-cloud variables are restricted to data points with a liquid water content of more than $1\ \mathrm{g\,kg^{-1}}$ in both model and observations.

3.2 Cloud droplet number concentrations

Figure 2 shows median in situ measurements of CDNC during flights and the median CDNC values from the entire nested model domain corresponding to the flight. Modeled and measured CDNC match for lower values of 200 $\mathrm{cm^{-3}}$ (AC09), but diverge for higher values. There is a linear relationship between WRF-Chem results and observations, albeit below the one-to-one line, leading to a factor of two of underestimation of CDNC for the most polluted case investigated (AC12 with about 750 $\mathrm{cm^{-3}}$ observed).

3.3 Variability in modeled r_{eff} profiles

All WRF-Chem modeled r_{eff} data from the ten nested domains was combined and binned by cloud-base CCN concentration (Figure 3). Cloud-base CCN is defined as the modeled CCN concentration at 0.5 $\%$ supersaturation directly below the lowest cloudy pixel in a model column.

The binning of r_{eff} profiles shows that the modeled profiles correspond to theoretical expectations; clouds with more available CCNs have a r_{eff} profile that is shifted towards smaller values relative to those with fewer available CCNs. The response

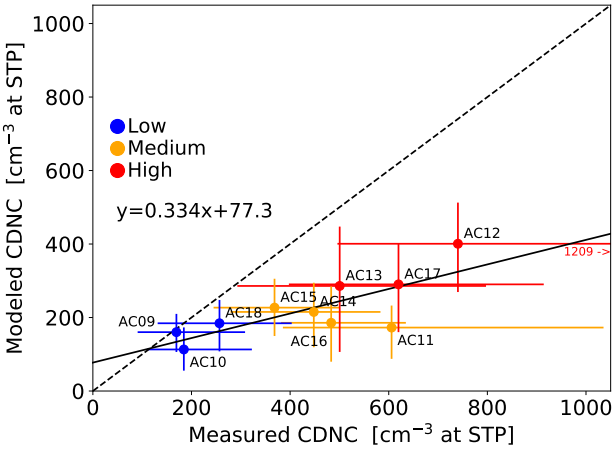

Figure 2. Median cloud droplet number concentration from the WRF domain and in situ measurements. The colors correspond to the CCN level labels in Table 1. Error bars depict the interquartile range (25 - 75% of all values). The equation describes the (solid black) regression line. The dashed black line is a 1-to-1 line for reference. STP refers to standard temperature (273.15K) and pressure (1000hPa).

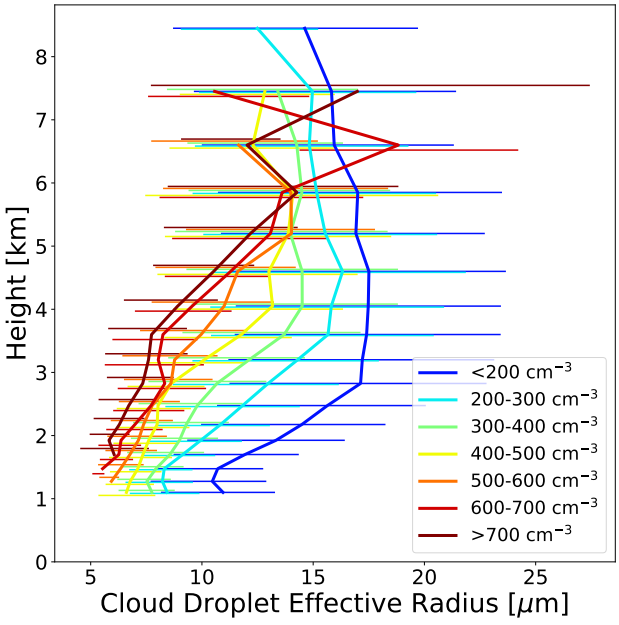

Figure 3. WRF-Chem simulated median cloud drop effective radius vertical profiles from all nested domain output during the study period, binned by below-cloud CCN concentration [cm^{-3} at STP]. Error bars represent the 20th to 80th percentile for each level and are offset vertically for readability.

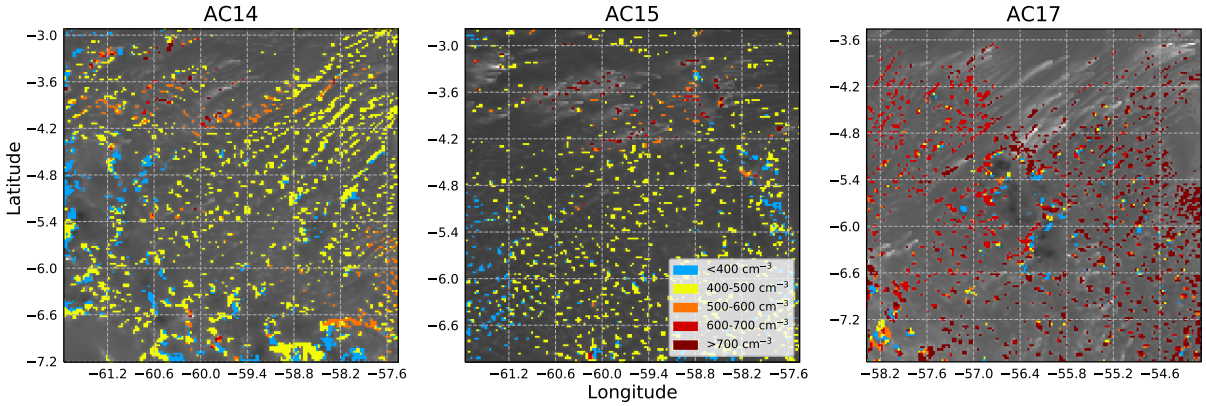

Figure 4. Spatial variability in modeled concentration of CCN at cloud base on three days (at 18Z) for the entire nested domain. Modelled aerosol optical depth (AOD) is shown as grey shading in the background, with brighter colors indicating higher AOD values. CCN concentrations are only shown where clouds were present.

to CCN concentration saturates in the model around 500-600 cm^{-3}, indicating that biomass burning effects will be nonlinear and strongest in relatively clean conditions. We did not find such a saturation effect for CDNC (Figure 2). Between 2 - 4 km above sea level, where the most model clouds occur, the slope of the profile also scales with available CCNs. The radius grows quickly with height to a maximum r_{eff} under low CCN (clean) conditions, whereas under high CCN (polluted) conditions the radius does not reach a maximum until much higher in the atmosphere. The profiles reach a maximum and then remain roughly constant at higher elevations. Under clean conditions, the maximum r_{eff} is larger and is reached at lower elevations. Profiles for the cleanest conditions also exhibit the largest maximum median r_{eff} of about 17 $\mu\mathrm{m}$.

3.4 Comparison of modeled and observed r_{eff} profiles

WRF-Chem modelled r_{eff} profiles were compared to remote-sensed and in situ measured profiles. In Figure 4 we show snapshots of the spatial variability of modeled CCN concentrations at cloud base for three different days. This figure demonstrates the influence of the fires on the regional CCN concentrations and highlights the CCN variability at large and small scales. Three dimensional CCN fields were simulated, but below-cloud concentrations (i.e. CCN concentration below the lowest cloudy point in a column) are most relevant for cloud droplet size. Figure 5 a-c then shows r_{eff} profiles derived from specMACS from two-minute cloud scenes on these three days, below-cloud-CCN binned WRF r_{eff} profiles from three hours near the specMACS data collection time, and all in situ r_{eff} profile measurements within the nested model domain. Figure 5 d-f shows the known modeled and in situ CDNCs. No CDNC are available for the specMACS observations since those data are remotely sensed.

Note that this is an approximate comparison, as no exact colocation can be expected between in situ and remote-sensed clouds, and we cannot compare individual modelled clouds directly to observed ones. Visual inspection of the slope and

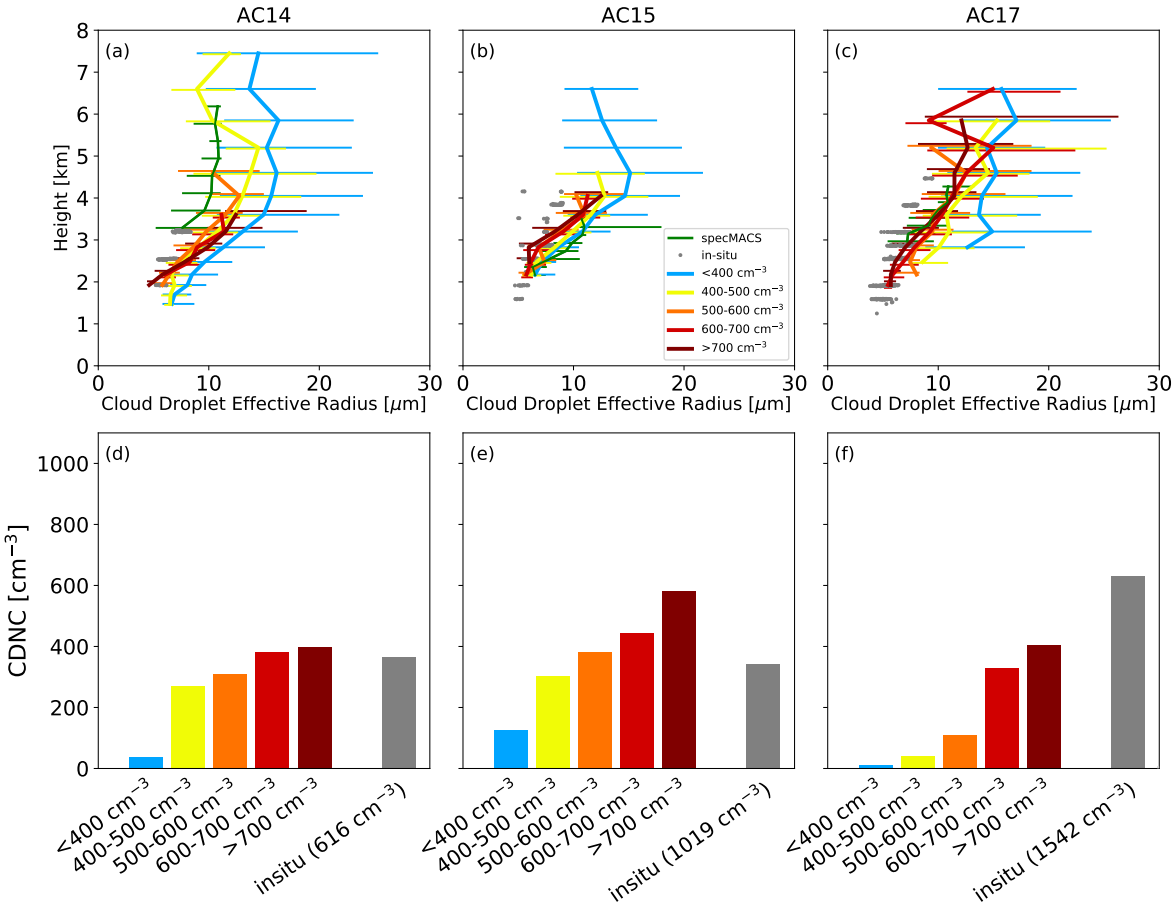

Figure 5. r_{eff} profiles and associated cloud droplet number concentration (CDNC) on three days during the field campaign. (a-c) show a comparison of median WRF-Chem, specMACS, and insitu r_{eff} profiles. (d-f) show the "true" below-cloud CCN-binned CDNC from WRF-Chem simulations and CDNC from in situ cloud profiling. Average in situ CCN concentrations (below 2 km) are presented in the bar label for the in situ derived N_{a}. See Section 3.1 for details regarding the definition of "average".

magnitude of median r_{eff} profiles measured by specMACS suggests that they match reasonably well to those from WRF-Chem, though in situ r_{eff} tend to be smaller than both the modeled or the ones retrieved by specMACS for all three cases investigated here.

The relatively small differences between r_{eff} profiles at larger CDNC are expected because the theoretical relationship between r_{eff} and CDNC is $r_{\mathrm{eff}} \sim (\frac{LWC}{CDNC})^{1/3}$ (Morrison and Gettelman, 2008). A linear relationship between LWC and CDNC therefore results in saturation of r_{eff}. However, at what CDNC this saturation occurs is not equally well described.

3.5 Number of activated cloud condensation nuclei at cloud base

As a more quantitative comparison of the different profiles, the number of activated CCNs at cloud base (N_{a}) were derived for each profile based on the methodology proposed in Freud et al. (2011). Braga et al. (2017a) already showed a comparison against in-situ measurements, which we use as a starting point here for an evaluation against remote sensing and regional model results. For the same three days as in Figure 5, Figure 6 a-c shows the regressions between adiabatic liquid water content (LWC_{a}) and mean volume radius (r_{v}) that result (using Eq. 2) in the calculated $N_{\mathrm{a,calc}}$ values shown in Figure 6 d-f. LWC_{a} for the modeled profiles was calculated in model clouds at the same points as used for the r_{eff} values. For specMACS, a nested domain averaged LWC_{a} profile was used since the below-cloud CCN is unknown for those measurements. The same profile was used for the in situ LWC_{a} to allow for direct comparisons. Only the increasing portion of the WRF-Chem profiles were used for the fits in Figure 6 a-c; points above the first decrease that occurs above 4 km are excluded. The known CDNCs (Figure 5) and calculated N_{a} (Figure 6) matched well given that CDNC is being viewed as equivalent to N_{a}, although N_{a} is an upper limit for CDNC since CDNC can be influenced by processes like collision and coalescence. A direct comparison of the true and derived CDNC are shown in Figure 7. This comparison demonstrates the effectiveness of the Freud et al. (2011) method for model data. The relationship is linear, but there is a systematic positive bias of derived CDNC. The factor of 0.7 as taken from the literature may be an underestimation for the modeled clouds. Sensitivity of the derivation to cloud base height may explain why using modeled LWC_{a} resulted in high derived CDNC for two of the in situ derivations. Another contributor could be the high low-level CCN concentrations that were not reached in the model and in part by the use of an average model LWC_{a} rather than a "true" LWC_{a}. Even though $N_{\mathrm{a,WRF}}$ and $N_{\mathrm{a,calc}}$ do not match exactly, general trends are captured. The N_{a} derived from the specMACS r_{eff} profiles ($N_{\mathrm{a,spec}}$) fall within the range of modeled CDNCs (Figure 6 d-f). Compared to modeled CDNCs, specMACS-derived $N_{\mathrm{a,spec}}$ are relatively high, low, and central for AC14, AC15, and AC17, respectively.

With the available data it is not possible to know the aerosol or below-cloud properties for the clouds sampled by specMACS. We suggest, however, that we can use the model results to deduce that the specMACS observed relatively polluted clouds during AC14 (Figure 6 a,d), relatively clean clouds during AC15 (Figure 6 b,e), and medium polluted clouds during AC17 (Figure 6 c/f). The N_{a} derived from the in situ profiles is higher than the others. While the calculated N_{a} depends on the theoretical adabatic liquid water content (LWC_{a}), the measured LWC might in fact be lower. This finding should be explored further but is out of scope of this work.

3.6 Discussion

Modeled r_{eff} tended to be larger than in situ measurements of r_{eff}. Subsequently, directly modeled and model-derived CNDC concentrations were lower than in situ measurements and derivations. Partly, these differences can be accounted for by the low modeled CCN concentrations (Figure 2). However, the 20^{th} to 80^{th} percentile range of modeled profiles with high below-cloud CCNs do overlap with the in situ data. The modeled r_{eff} profiles began to saturate around 500 cm^{-3} at STP below-cloud CCN, with only small differences at higher concentrations (Figure 3), meaning that the modeled cloud albedo or Twomey effect saturates at approximately that concentration. A sensitivity study in which we artificially doubled the amount of biomass

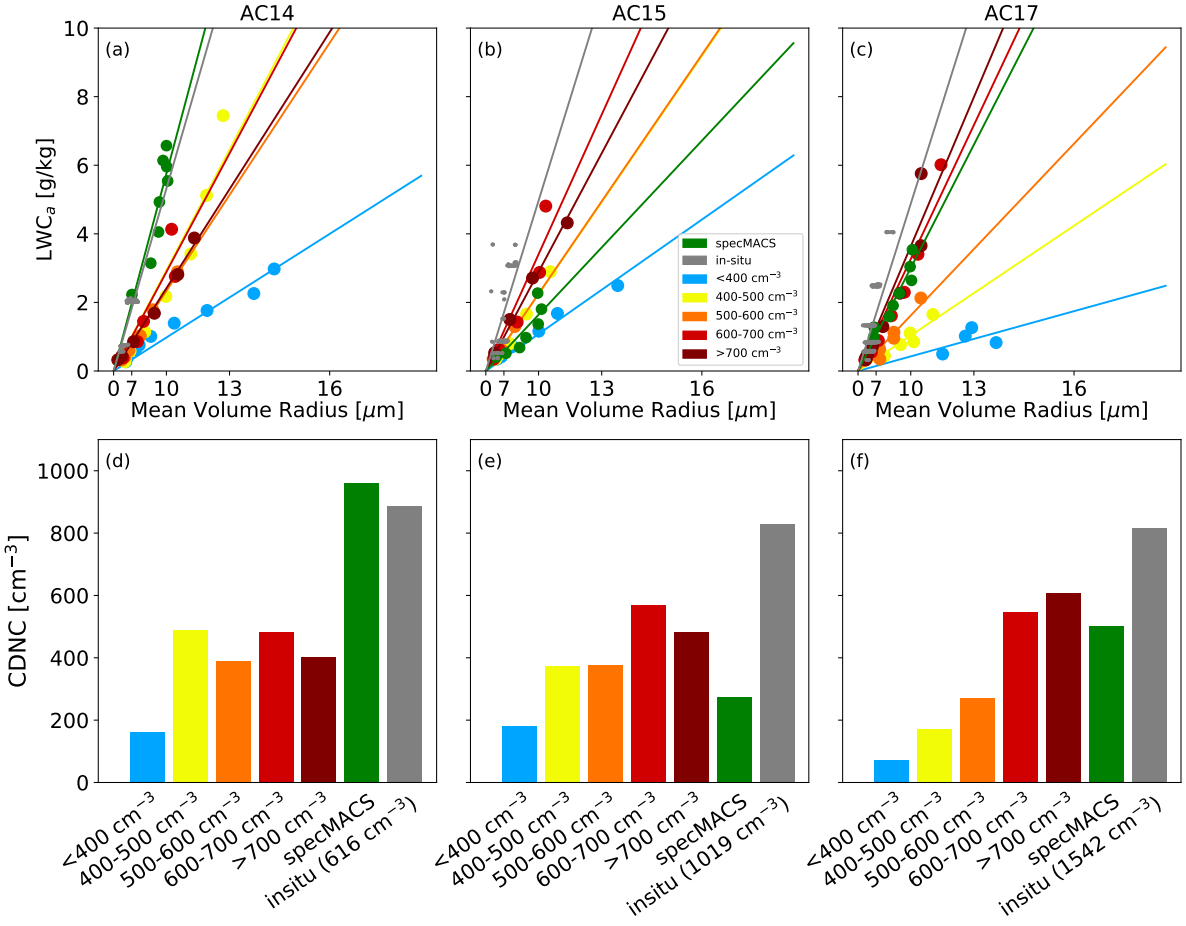

Figure 6. Derived cloud droplet number concentration (CDNC) on three days during the field campaign. (a-c) show the regressions between mean volume radius and adiabatic liquid water content (LWC_a) used to derive the CDNC as shown in (d-f). Average in situ CCN concentrations below 2 km are shown below the in situ derived N_a. (d-f) were derived from the slopes in (a-c), whereas Figure 5 d-f were more directly determined.

burning emissions showed the same saturation in modelled r_{eff}, further corroborating our findings. The concentration of around 500 cm^{-3} at STP below-cloud CCN is well below the CCN concentrations characteristic of the dry season in the southern half of the Amazon Basin, which are typically in the range of 1000 to 7000 cm^{-3} (Andreae et al., 2004; Andreae, 2009; Andreae et al., 2018). No such saturation was observed in the evaluation of modelled CDNC.

Increased model spatial resolution could potentially provide better agreement for these high-pollution situations, but a variety of hurdles (input data resolution of emissions and static data like land use, vegetation cover and topography, model formulation of turbulence, statistical methods for output analysis) need to be overcome before reliable simulations at higher resolution are feasible. The horizontal grid resolution of 3 km is at the fine end of what regional modeling systems were designed for,

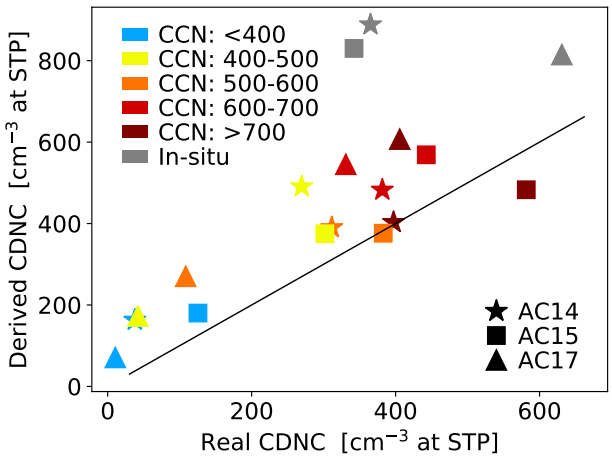

Figure 7. Comparison of real (i.e. CDP and CAS measured) CDNC with CDNC as derived using the Freud et al. (2011) method. Real CDNC for model data are average modeled CDNC in the model domain. Symbols indicate date, colors indicate model bin or in situ data. The one to one line is for reference. These are the same data as Figure 5 d-f and Figure 6 d-f.

reaching for 'terra incognita' (Wyngaard, 2004) in terms of resolution. Sensitivity simulations in which we simply increased the horizontal and/or vertical resolution by a factor of two did not lead to improved agreement with observations.

More complex parameterizations of cloud microphysics, such as spectral bin microphysics (e.g. Grützun et al., 2008; Khain and Sednev, 1996), have been developed and used before in case studies. Such more complex parameterisations might improve the representation of the cloud droplet size spectra and hence also modelled r_{eff}. Such parameterisations are, however, still computationally too expensive to be used on a regular basis or in the context of a climate study.

Estimating the radiative forcing due to biomass burning is of central importance to evaluate its impact on the climate system. Calculating the top of atmosphere radiative forcing leads to an campaign average daytime cooling of -0.9 W m^{-2} (not shown), which is comparable to previous estimates (e.g. Archer-Nicholls et al., 2016) and shows that our model behaves similar to existing studies. However, given the demonstrated lack of skill of the modeling system in representing the very strong CCN perturbations due to biomass burning, we refrained from further exploring their climate impacts.

We deem our modeling study is representative for other regional scale chemistry-transport modeling studies of aerosol-cloud interactions of convective clouds in situations strongly affected by biomass burning (e.g., Martins et al., 2009; Wu et al., 2011; Archer-Nicholls et al., 2016). WRF-Chem is a widely used modeling system and similar to other regional modeling systems. Our setup contains state of the art representations of clouds, aerosols, and aerosol-cloud interactions because we used a two-moment cloud microphysics scheme with a sectional aerosol module, and the cloud activation scheme of Abdul-Razzak and Ghan (2000).

Comparisons between entire model domains and in situ measurements are inherently difficult since the exact measured clouds will never be realistically simulated due to the randomness of modeled clouds and the difference in scales. There are

a variety of challenges involved with this comparison. However, especially at high CCN, the model overestimates r_{eff} and, therefore, underestimates N_{a}. The specMACS data experience similar comparison difficulties since each set only spans a cloud scene ($\sim$50 km) over a short time ($\sim$2 $\mathrm{minutes}$). However, the retrieved r_{eff} profiles still fall within the in situ measurements and the model output. Profile values derived from specMACS measurements also tend to be smaller than the data from in situ sampling, which is expected based on previous tests (Ewald et al., 2016).

We have demonstrated that the method by Freud et al. (2011) to derive cloud base CDNC from r_{eff} observations can successfully be applied in conjunction with simulated clouds to derive N_{a} from remotely sensed hyperspectral data of the specMACS instrument. The method is limited by its high sensitivity at low N_{a} due to the mathematical nature of the slope (i.e. steep slopes in Figure 6 a-c) and we are unable to verify its accuracy with the available data. It also uses an average mixing factor that may vary for the cloud scenes measured my specMACS. However, using Figure 7 as a guide to the accuracy of the method, the uncertainties appear to be smaller than those from satellite retrievals, which are about 78 $\%$ at the pixel level (Grosvenor et al., 2018). We therefore propose that model results can be used to differentiate specMACS observations into clean and polluted conditions, which will need to be verified in future studies.

4 Conclusions

Aerosol-cloud interactions have been the focus of field campaigns and measurement development due to the large associated model uncertainty. Here we used novel observations taken on board the HALO aircraft during the ACRIDICON-CHUVA field campaign to evaluate cloud representation in a numerical model to aid in reducing this uncertainty. We demonstrated that we can reproduce realistic cloud properties (i.e., cloud droplet effective radius profiles) with a regional online-coupled chemistry-transport model at convection-permitting scales for the Amazon region during the biomass burning season. As expected by theory, the number of CCN at cloud base has a major influence on cloud droplet size and the shape of the effective radius vertical profile. Increasing CCN leads to decreasing cloud droplet sizes, and we could show that both model and observations exhibit quantitatively similar behavior. We also observed a saturation effect at high aerosol concentrations (number concentration of CCN larger than 500 $\mathrm{cm}^{-3}\,\mathrm{at\,STP}$) in the model, above which we find no further change in modelled effective droplet size or the shape of the droplet size profile. Our model results are in disagreement with observations of microphysical effects at much higher aerosol loading from previous campaigns (Reid et al., 1999; Andreae et al., 2004) and from the ACRIDICON-CHUVA campaign (Braga et al., 2017b). This finding casts doubt on the validity of using a setup like ours for regional scale modeling studies of the cloud albedo effect (Twomey, 1991) of convective clouds for biomass burning situations at high CCN concentrations. Although we only tested one microphysics scheme, we demonstrated that a modern, complex parameterization does not imply accurate representation of cloud microphysical properties and suggest that calculations of the radiative forcing of these phenomena would therefore be unreliable. We conclude that there is a need for further model-measurement comparisons to better understand model biases.

Code and data availability. Model data, the source code used in the evaluation, as well as all observational data, are available from the authors upon request.

Author contributions. PP ran the simulations and conducted the analysis under the supervision of CK and TZ. PP, TZ and CK wrote the manuscript, with input from BM, MA, DR, RW and MW. MA, CP, MP, UP, DR, RW and MW contributed through fruitful discussions. FE, TKo, TJ, TKl, CM, SM, CP, MP, CV and RW provided measurements essential for this manuscript.

Competing interests. The authors declare no competing interests.

Acknowledgements. We thank the Leibniz Supercomputing Centre (LRZ) of the Bavarian Academy of Sciences and Humanities (BAdW) for the support and provisioning of computing infrastructure essential to this publication. We acknowledge use of the WRF-Chem preprocessor tools anthro_emiss, exo_coldens, fire_emiss, megan_bio_emiss, mozbc and wesely provided by the Atmospheric Chemistry Observations and Modeling Lab (ACOM) of NCAR. We acknowledge use of MOZART-4 global model output available at http://www.acom.ucar.edu/wrf-chem/mozart.shtml (last accessed 24.07.2018). We thank National Centers for Environmental Prediction for making Global Forecasting System data publically available. We also thank DLR for access to the HALO database for all in situ data used in this study. This work was supported by the Max Planck Society, the DFG (Deutsche Forschungsgemeinschaft, German Research Foundation) Priority Program SPP 1294, the German Aerospace Center (DLR), the FAPESP (São Paulo Research Foundation) Grants 2009/15235-8 and 2013/05014-0, and a wide range of other institutional partners.

References

Abdul-Razzak, H. and Ghan, S. J.: A parameterization of aerosol activation: 2. Multiple aerosol types, Journal of Geophysical Research: Atmospheres, 105, 6837–6844, https://doi.org/10.1029/1999JD901161, 2000.

Abdul-Razzak, H. and Ghan, S. J.: A parameterization of aerosol activation 3. Sectional representation, Journal of Geophysical Research: Atmospheres, 107, https://doi.org/10.1029/2001JD000483, 2002.

Albrecht, B. A.: Aerosols, cloud microphysics, and fractional cloudiness, Science, 245, 1227–1230, 1989.

Andreae, M. O.: Correlation between cloud condensation nuclei concentration and aerosol optical thickness in remote and polluted regions, Atmospheric Chemistry and Physics, 9, 543–556, https://doi.org/10.5194/acp-9-543-2009, https://www.atmos-chem-phys.net/9/543/2009/, 2009.

Andreae, M. O., Rosenfeld, D., Artaxo, P., Costa, A., Frank, G., Longo, K., and Silva-Dias, M.: Smoking rain clouds over the Amazon, Science, 303, 1337–1342, 2004.

Andreae, M. O., Afchine, A., Albrecht, R., Holanda, B. A., Artaxo, P., Barbosa, H. M. J., Borrmann, S., Cecchini, M. A., Costa, A., Dollner, M., Fütterer, D., Järvinen, E., Jurkat, T., Klimach, T., Konemann, T., Knote, C., Krämer, M., Krisna, T., Machado, L. A. T., Mertes, S., Minikin, A., Pöhlker, C., Pöhlker, M. L., Pöschl, U., Rosenfeld, D., Sauer, D., Schlager, H., Schnaiter, M., Schneider, J., Schulz, C., Spanu, A., Sperling, V. B., Voigt, C., Walser, A., Wang, J., Weinzierl, B., Wendisch, M., and Ziereis, H.: Aerosol characteristics and particle production in the upper troposphere over the Amazon Basin, Atmospheric Chemistry and Physics, 18, 921–961, https://doi.org/10.5194/acp-18-921-2018, https://www.atmos-chem-phys.net/18/921/2018/, 2018.

Archer-Nicholls, S., Lowe, D., Schultz, D. M., and McFiggans, G.: Aerosol–radiation–cloud interactions in a regional coupled model: the effects of convective parameterisation and resolution, Atmospheric Chemistry and Physics, 16, 5573, 2016.

Barnard, J. C., Fast, J. D., Paredes-Miranda, G., Arnott, W. P., and Laskin, A.: Technical Note: Evaluation of the WRF-Chem "Aerosol Chemical to Aerosol Optical Properties" Module using data from the MILAGRO campaign, Atmospheric Chemistry and Physics, 10, 7325–7340, https://doi.org/10.5194/acp-10-7325-2010, 2010.

Baumgardner, D., Brenguier, J., Bucholtz, A., Coe, H., DeMott, P., Garrett, T., Gayet, J., Hermann, M., Heymsfield, A., Korolev, A., et al.: Airborne instruments to measure atmospheric aerosol particles, clouds and radiation: A cook's tour of mature and emerging technology, Atmospheric Research, 102, 10–29, 2011.

Baumgardner, D., Newton, R., Krämer, M., Meyer, J., Beyer, A., Wendisch, M., and Vochezer, P.: The Cloud Particle Spectrometer with Polarization Detection (CPSPD): A next generation open-path cloud probe for distinguishing liquid cloud droplets from ice crystals, Atmospheric Research, 142, 2–14, 2014.

Braga, R. C., Rosenfeld, D., Weigel, R., Jurkat, T., Andreae, M. O., Wendisch, M., Pöhlker, M. L., Klimach, T., Pöschl, U., Pöhlker, C., Voigt, C., Mahnke, C., Borrmann, S., Albrecht, R. I., Molleker, S., Vila, D. A., Machado, L. A. T., and Artaxo, P.: Comparing parameterized versus measured microphysical properties of tropical convective cloud bases during the ACRIDICON–CHUVA campaign, Atmospheric Chemistry and Physics, 17, 7365–7386, https://doi.org/10.5194/acp-17-7365-2017, 2017a.

Braga, R. C., Rosenfeld, D., Weigel, R., Jurkat, T., Andreae, M. O., Wendisch, M., Pöschl, U., Voigt, C., Mahnke, C., Borrmann, S., et al.: Further evidence for CCN aerosol concentrations determining the height of warm rain and ice initiation in convective clouds over the Amazon basin, Atmospheric Chemistry and Physics, 17, 14 433–14 456, 2017b.

Brioude, J., Cooper, O., Feingold, G., Trainer, M., Freitas, S., Kowal, D., Ayers, J., Prins, E., Minnis, P., McKeen, S., et al.: Effect of biomass burning on marine stratocumulus clouds off the California coast, Atmospheric Chemistry and Physics, 9, 8841–8856, 2009.

Chapman, E. G., Gustafson Jr, W., Easter, R. C., Barnard, J. C., Ghan, S. J., Pekour, M. S., and Fast, J. D.: Coupling aerosol-cloud-radiative processes in the WRF-Chem model: Investigating the radiative impact of elevated point sources, Atmospheric Chemistry and Physics, 9, 945–964, 2009.

Emmons, L. K., Walters, S., Hess, P. G., Lamarque, J.-F., Pfister, G. G., Fillmore, D., Granier, C., Guenther, A., Kinnison, D., Laepple, T., Orlando, J., Tie, X., Tyndall, G., Wiedinmyer, C., Baughcum, S. L., and Kloster, S.: Description and evaluation of the Model for Ozone and Related chemical Tracers, version 4 (MOZART-4), Geoscientific Model Development, 3, 43–67, https://doi.org/10.5194/gmd-3-43-2010, 2010.

Ewald, F., Kölling, T., Baumgartner, A., Zinner, T., and Mayer, B.: Design and characterization of specMACS, a multipurpose hyperspectral cloud and sky imager, Atmospheric Measurement Techniques, pp. 2015–2042, 2016.

Ewald, F., Zinner, T., Kölling, T., and Mayer, B.: Remote Sensing of Cloud Droplet Radius Profiles using solar reflectance from cloud sides. Part I: Retrieval development and characterization, Atmospheric Measurement Techniques Discussions, 2018, 1–35, https://doi.org/10.5194/amt-2018-234, 2018.

Fast, J. D., Gustafson Jr, W. I., Easter, R. C., Zaveri, R. A., Barnard, J. C., Chapman, E. G., Grell, G. A., and Peckham, S. E.: Evolution of ozone, particulates, and aerosol direct radiative forcing in the vicinity of Houston using a fully coupled meteorology-chemistry-aerosol model, Journal of Geophysical Research: Atmospheres, 111, 2006.

Feingold, G., Jiang, H., and Harrington, J. Y.: On smoke suppression of clouds in Amazonia, Geophysical Research Letters, 32, 2005.

Flamant, C., Knippertz, P., Fink, A. H., Akpo, A., Brooks, B., Chiu, C. J., Coe, H., Danuor, S., Evans, M., Jegede, O., et al.: The Dynamics–Aerosol–Chemistry–Cloud Interactions in West Africa Field Campaign: Overview and Research Highlights, Bulletin of the American Meteorological Society, 99, 83–104, 2018.

Freud, E., Rosenfeld, D., and Kulkarni, J.: Resolving both entrainment-mixing and number of activated CCN in deep convective clouds, Atmospheric Chemistry and Physics, 11, 12 887–12 900, 2011.

Ghan, S., Wang, M., Zhang, S., Ferrachat, S., Gettelman, A., Griesfeller, J., Kipling, Z., Lohmann, U., Morrison, H., Neubauer, D., et al.: Challenges in constraining anthropogenic aerosol effects on cloud radiative forcing using present-day spatiotemporal variability, Proceedings of the National Academy of Sciences, 113, 5804–5811, 2016.

Gonçalves, W., Machado, L., and Kirstetter, P.-E.: Influence of biomass aerosol on precipitation over the Central Amazon: an observational study, Atmospheric Chemistry and Physics, 15, 6789–6800, 2015.

Grell, G. A., Peckham, S. E., Schmitz, R., McKeen, S. A., Frost, G., Skamarock, W. C., and Eder, B.: Fully coupled "online" chemistry within the WRF model, Atmospheric Environment, 39, 6957–6975, 2005.

Grosvenor, D. P., Sourdeval, O., Zuidema, P., Ackerman, A., Alexandrov, M. D., Bennartz, R., Boers, R., Cairns, B., Chiu, J. C., Christensen, M., Deneke, H., Diamond, M., Feingold, G., Fridlind, A., Hünerbein, A., Knist, C., Kollias, P., Marshak, A., McCoy, D., Merk, D., Painemal, D., Rausch, J., Rosenfeld, D., Russchenberg, H., Seifert, P., Sinclair, K., Stier, P., van Diedenhoven, B., Wendisch, M., Werner, F., Wood, R., Zhang, Z., and Quaas, J.: Remote Sensing of Droplet Number Concentration in Warm Clouds: A Review of the Current State of Knowledge and Perspectives, Reviews of Geophysics, 56, 409–453, https://doi.org/10.1029/2017RG000593, 2018.

Grützun, V., Knoth, O., and Simmel, M.: Simulation of the influence of aerosol particle characteristics on clouds and precipitation with LM-SPECS: Model description and first results, Atmospheric Research, 90, 233 – 242, https://doi.org/https://doi.org/10.1016/j.atmosres.2008.03.002, http://www.sciencedirect.com/science/article/pii/S0169809508000604, 17th International Conference on Nucleation and Atmospheric Aerosols, 2008.

Guenther, A., Karl, T., Harley, P., Wiedinmyer, C., Palmer, P., and Geron, C.: Estimates of global terrestrial isoprene emissions using MEGAN (Model of Emissions of Gases and Aerosols from Nature), Atmospheric Chemistry and Physics, 6, 3181–3210, 2006.

Gustafson Jr, W. I., Chapman, E. G., Ghan, S. J., Easter, R. C., and Fast, J. D.: Impact on modeled cloud characteristics due to simplified treatment of uniform cloud condensation nuclei during NEAQS 2004, Geophysical Research Letters, 34, 2007.

IPCC: Climate Change 2014: Synthesis Report. Contribution of Working Groups I, II and III to the Fifth Assessment Report of the Intergovernmental Panel on Climate Change, IPCC, Geneva, Switzerland, 2014.

Jäkel, E., Wendisch, M., Krisna, T. C., Ewald, F., Kölling, T., Jurkat, T., Voigt, C., Cecchini, M. A., Machado, L. A. T., Afchine, A., Costa, A., Krämer, M., Andreae, M. O., Pöschl, U., Rosenfeld, D., and Yuan, T.: Vertical distribution of the particle phase in tropical deep convective clouds as derived from cloud-side reflected solar radiation measurements, Atmospheric Chemistry and Physics, 17, 9049–9066, https://doi.org/10.5194/acp-17-9049-2017, 2017.

Janssens-Maenhout, G., Dentener, F., Van Aardenne, J., Monni, S., Pagliari, V., Orlandini, L., Klimont, Z., Kurokawa, J.-i., Akimoto, H., Ohara, T., et al.: EDGAR-HTAP: a harmonized gridded air pollution emission dataset based on national inventories, European Commission Joint Research Centre Institute for Environment and Sustainability. JRC 68434 UR 25229 EUR 25229, ISBN 978-92-79-23123-0, 2012.

Järvinen, E., Schnaiter, M., Mioche, G., Jourdan, O., Shcherbakov, V. N., Costa, A., Afchine, A., Krämer, M., Heidelberg, F., Jurkat, T., et al.: Quasi-spherical ice in convective clouds, Journal of the Atmospheric Sciences, 73, 3885–3910, 2016.

Kaufman, Y. J. and Fraser, R. S.: The effect of smoke particles on clouds and climate forcing, Science, 277, 1636–1639, 1997.

Kaufman, Y. J. and Nakajima, T.: Effect of Amazon smoke on cloud microphysics and albedo-analysis from satellite imagery, Journal of Applied Meteorology, 32, 729–744, 1993.

Khain, A., Rosenfeld, D., and Pokrovsky, A.: Aerosol impact on the dynamics and microphysics of deep convective clouds, Quarterly Journal of the Royal Meteorological Society: A journal of the atmospheric sciences, applied meteorology and physical oceanography, 131, 2639–2663, 2005.

Khain, A. P. and Sednev, I.: Simulation of precipitation formation in the Eastern Mediterranean coastal zone using a spectral microphysics cloud ensemble model, Atmospheric Research, 43, 77 – 110, https://doi.org/https://doi.org/10.1016/S0169-8095(96)00005-1, http://www.sciencedirect.com/science/article/pii/S0169809596000051, 1996.

Kleine, J., Voigt, C., Sauer, D., Schlager, H., Scheibe, M., Jurkat-Witschas, T., Kaufmann, S., Kärcher, B., and Anderson, B. E.: In Situ Observations of Ice Particle Losses in a Young Persistent Contrail, Geophysical Research Letters, 45, 13,553–13,561, https://doi.org/10.1029/2018GL079390, 2018.

Knote, C., Hodzic, A., Jimenez, J. L., Volkamer, R., Orlando, J. J., Baidar, S., Brioude, J., Fast, J., Gentner, D. R., Goldstein, A. H., Hayes, P. L., Knighton, W. B., Oetjen, H., Setyan, A., Stark, H., Thalman, R., Tyndall, G., Washenfelder, R., Waxman, E., and Zhang, Q.: Simulation of semi-explicit mechanisms of SOA formation from glyoxal in aerosol in a 3-D model, Atmospheric Chemistry and Physics, 14, 6213–6239, https://doi.org/10.5194/acp-14-6213-2014, 2014.

Knote, C., Hodzic, A., and Jimenez, J. L.: The effect of dry and wet deposition of condensable vapors on secondary organic aerosols concentrations over the continental US, Atmospheric Chemistry and Physics, 15, 1–18, https://doi.org/10.5194/acp-15-1-2015, 2015.

Krüger, M. L., Mertes, S., Klimach, T., Cheng, Y. F., Su, H., Schneider, J., Andreae, M. O., Pöschl, U., and Rose, D.: Assessment of cloud supersaturation by size-resolved aerosol particle and cloud condensation nuclei (CCN) measurements, Atmospheric Measurement Techniques, 7, 2615–2629, https://doi.org/10.5194/amt-7-2615-2014, 2014.

Lance, S., Brock, C., Rogers, D., and Gordon, J. A.: Water droplet calibration of the Cloud Droplet Probe (CDP) and in-flight performance in liquid, ice and mixed-phase clouds during ARCPAC, Atmospheric Measurement Techniques, 3, 1683–1706, 2010.

Levin, Z., Teller, A., Ganor, E., and Yin, Y.: On the interactions of mineral dust, sea-salt particles, and clouds: A measurement and modeling study from the Mediterranean Israeli Dust Experiment campaign, Journal of Geophysical Research: Atmospheres, 110, 2005.

Lin, J. C., Matsui, T., Pielke Sr, R., and Kummerow, C.: Effects of biomass-burning-derived aerosols on precipitation and clouds in the Amazon Basin: A satellite-based empirical study, Journal of Geophysical Research: Atmospheres, 111, 2006.

Malavelle, F. F., Haywood, J. M., Jones, A., Gettelman, A., Clarisse, L., Bauduin, S., Allan, R. P., Karset, I. H. H., Kristjánsson, J. E., Oreopoulos, L., et al.: Strong constraints on aerosol–cloud interactions from volcanic eruptions, Nature, 546, 485, 2017.

Marshak, A., Platnick, S., Várnai, T., Wen, G., and Cahalan, R. F.: Impact of three-dimensional radiative effects on satellite retrievals of cloud droplet sizes, Journal of Geophysical Research: Atmospheres, 111, 2006.

Martin, S. T., Artaxo, P., Machado, L., Manzi, A., Souza, R., Schumacher, C., Wang, J., Biscaro, T., Brito, J., Calheiros, A., et al.: The Green Ocean Amazon experiment (GoAmazon2014/5) observes pollution affecting gases, aerosols, clouds, and rainfall over the rain forest, Bulletin of the American Meteorological Society, 98, 981–997, 2017.

Martins, J. A., Silva Dias, M. A. F., and Gonçalves, F. L. T.: Impact of biomass burning aerosols on precipitation in the Amazon: A modeling case study, Journal of Geophysical Research: Atmospheres, 114, https://doi.org/10.1029/2007JD009587, 2009.

Martins, J. V., Marshak, A., Remer, L., Rosenfeld, D., Kaufman, Y., Fernandez-Borda, R., Koren, I., Correia, A. L., Zubko, V., and Artaxo, P.: Remote sensing the vertical profile of cloud droplet effective radius, thermodynamic phase, and temperature, Atmospheric Chemistry and Physics, 11, 9485–9501, 2011.

McCoy, D. T. and Hartmann, D. L.: Observations of a substantial cloud-aerosol indirect effect during the 2014–2015 Baroarbunga-Veioivotn fissure eruption in Iceland, Geophysical Research Letters, 42, 10–409, 2015.

Morrison, H. and Gettelman, A.: A new two-moment bulk stratiform cloud microphysics scheme in the Community Atmosphere Model, version 3 (CAM3). Part I: Description and numerical tests, Journal of Climate, 21, 3642–3659, 2008.

Morrison, H., Curry, J., and Khvorostyanov, V.: A new double-moment microphysics parameterization for application in cloud and climate models. Part I: Description, Journal of the Atmospheric Sciences, 62, 1665–1677, 2005.

Pöhlker, M. L., Ditas, F., Saturno, J., Klimach, T., Hrabě de Angelis, I., Araùjo, A. C., Brito, J., Carbone, S., Cheng, Y., Chi, X., Ditz, R., Gunthe, S. S., Holanda, B. A., Kandler, K., Kesselmeier, J., Könemann, T., Krüger, O. O., Lavrič, J. V., Martin, S. T., Mikhailov, E., Moran-Zuloaga, D., Rizzo, L. V., Rose, D., Su, H., Thalman, R., Walter, D., Wang, J., Wolff, S., Barbosa, H. M. J., Artaxo, P., Andreae, M. O., Pöschl, U., and Pöhlker, C.: Long-term observations of cloud condensation nuclei over the Amazon rain forest – Part 2: Variability and characteristics of biomass burning, long-range transport, and pristine rain forest aerosols, Atmospheric Chemistry and Physics, 18, 10 289–10 331, https://doi.org/10.5194/acp-18-10289-2018, 2018.

Reid, J. S., Hobbs, P. V., Rangno, A. L., and Hegg, D. A.: Relationships between cloud droplet effective radius, liquid water content, and droplet concentration for warm clouds in Brazil embedded in biomass smoke, Journal of Geophysical Research: Atmospheres, 104, 6145–6153, 1999.

Roberts, G. and Nenes, A.: A continuous-flow streamwise thermal-gradient CCN chamber for atmospheric measurements, Aerosol Science and Technology, 39, 206–221, 2005.

Rose, D., Gunthe, S., Mikhailov, E., Frank, G., Dusek, U., Andreae, M. O., and Pöschl, U.: Calibration and measurement uncertainties of a continuous-flow cloud condensation nuclei counter (DMT-CCNC): CCN activation of ammonium sulfate and sodium chloride aerosol particles in theory and experiment, Atmospheric Chemistry and Physics, 8, 1153–1179, 2008.

Rosenfeld, D.: TRMM observed first direct evidence of smoke from forest fires inhibiting rainfall, Geophysical Research Letters, 26, 3105–3108, 1999.

Rosenfeld, D., Williams, E., Andreae, M., Freud, E., Pöschl, U., and Rennó, N.: The scientific basis for a satellite mission to retrieve CCN concentrations and their impacts on convective clouds, Atmospheric Measurement Techniques, 5, 2039–2055, 2012.

Sassen, K., DeMott, P. J., Prospero, J. M., and Poellot, M. R.: Saharan dust storms and indirect aerosol effects on clouds: CRYSTAL-FACE results, Geophysical Research Letters, 30, 2003.

Schumann, U., Baumann, R., Baumgardner, D., Bedka, S. T., Duda, D. P., Freudenthaler, V., Gayet, J.-F., Heymsfield, A. J., Minnis, P., Quante, M., Raschke, E., Schlager, H., Vázquez-Navarro, M., Voigt, C., and Wang, Z.: Properties of individual contrails: a compilation of observations and some comparisons, Atmospheric Chemistry and Physics, 17, 403–438, https://doi.org/10.5194/acp-17-403-2017, 2017.

Seifert, A. and Beheng, K. D.: A two-moment cloud microphysics parameterization for mixed-phase clouds. Part 1: Model description, Meteorology and Atmospheric Physics, 92, 45–66, https://doi.org/10.1007/s00703-005-0112-4, https://doi.org/10.1007/s00703-005-0112-4, 2006.

Seinfeld, J. H., Bretherton, C., Carslaw, K. S., Coe, H., DeMott, P. J., Dunlea, E. J., Feingold, G., Ghan, S., Guenther, A. B., Kahn, R., et al.: Improving our fundamental understanding of the role of aerosol- cloud interactions in the climate system, Proceedings of the National Academy of Sciences, 113, 5781–5790, 2016.

Taylor, J. W., Haslett, S. L., Bower, K., Flynn, M., Crawford, I., Dorsey, J., Choularton, T., Connolly, P. J., Hahn, V., Voigt, C., et al.: Aerosol influences on low-level clouds in the West African monsoon, Atmos. Chem. Phys. Discuss., https://doi. org/10.5194/acp-2019-40, in review, 2019.

Ten Hoeve, J., Remer, L., and Jacobson, M.: Microphysical and radiative effects of aerosols on warm clouds during the Amazon biomass burning season as observed by MODIS: impacts of water vapor and land cover, Atmospheric Chemistry and Physics, 11, 3021–3036, 2011.

Thompson, G. and Eidhammer, T.: A Study of Aerosol Impacts on Clouds and Precipitation Development in a Large Winter Cyclone, Journal of the Atmospheric Sciences, 71, 3636–3658, https://doi.org/10.1175/JAS-D-13-0305.1, 2014.

Twomey, S.: Aerosols, clouds and radiation, Atmospheric Environment. Part A. General Topics, 25, 2435–2442, 1991.

Voigt, C., Schumann, U., Minikin, A., Abdelmonem, A., Afchine, A., Borrmann, S., Boettcher, M., Buchholz, B., Bugliaro, L., Costa, A., et al.: ML-CIRRUS: The airborne experiment on natural cirrus and contrail cirrus with the high-altitude long-range research aircraft HALO, Bulletin of the American Meteorological Society, 98, 271–288, 2017.

Wall, C., Zipser, E., and Liu, C.: An investigation of the aerosol indirect effect on convective intensity using satellite observations, Journal of the Atmospheric Sciences, 71, 430–447, 2014.

Weigel, R., Spichtinger, P., Mahnke, C., Klingebiel, M., Afchine, A., Petzold, A., Krämer, M., Costa, A., Molleker, S., Reutter, P., Szakáll, M., Port, M., Grulich, L., Jurkat, T., Minikin, A., and Borrmann, S.: Thermodynamic correction of particle concentrations measured by underwing probes on fast-flying aircraft, Atmospheric Measurement Techniques, 9, 5135–5162, https://doi.org/10.5194/amt-9-5135-2016, 2016.

Wendisch, M., Pöschl, U., Andreae, M. O., Machado, L. A., Albrecht, R., Schlager, H., Rosenfeld, D., Martin, S. T., Abdelmonem, A., Afchine, A., et al.: ACRIDICON–CHUVA campaign: Studying tropical deep convective clouds and precipitation over Amazonia using the new German research aircraft HALO, Bulletin of the American Meteorological Society, 97, 1885–1908, 2016.

Wiedinmyer, C., Akagi, S., Yokelson, R. J., Emmons, L., Al-Saadi, J., Orlando, J., and Soja, A.: The Fire INventory from NCAR (FINN): A high resolution global model to estimate the emissions from open burning, Geoscientific Model Development, 4, 625, 2011.

Wu, L., Su, H., and Jiang, J. H.: Regional simulations of deep convection and biomass burning over South America: 2. Biomass burning aerosol effects on clouds and precipitation, Journal of Geophysical Research: Atmospheres, 116, https://doi.org/10.1029/2011JD016106, 2011.

Wyngaard, J. C.: Toward Numerical Modeling in the "Terra Incognita", Journal of the Atmospheric Sciences, 61, 1816–1826, https://doi.org/10.1175/1520-0469(2004)061<1816:TNMITT>2.0.CO;2, 2004.

Zaveri, R. A., Easter, R. C., Fast, J. D., and Peters, L. K.: Model for simulating aerosol interactions and chemistry (MOSAIC), Journal of Geophysical Research: Atmospheres, 113, 2008.

Zhang, Y., Fu, R., Yu, H., Dickinson, R. E., Juarez, R. N., Chin, M., and Wang, H.: A regional climate model study of how biomass burning aerosol impacts land-atmosphere interactions over the Amazon, Journal of Geophysical Research: Atmospheres, 113, 2008.

Zinner, T., Marshak, A., Lang, S., Martins, J., and Mayer, B.: Remote sensing of cloud sides of deep convection: towards a three-dimensional retrieval of cloud particle size profiles, Atmospheric Chemistry and Physics, 8, 4741–4757, 2008.